ISSN:2229-6107

INTERNATIONAL JOURNAL OF PURE AND APPLIED SCIENCE & TECHNOLOGY

E-mail :
editor.ijpast@gmail.com
editor@ijpast.in

www.ijpast.in

INTERNATIONAL JOURNAL OF PURE AND APPLIED SCIENCE & TECHNOLOGY
IJPAST

ISSN 2229-6107www.ijpast.in
Vol 12 Issue 1 Mar 2022

New Cluster-Based MSE Equalizer with High Efficiency for M-QAM Satellite Channels

D. Ramu [1], A. Manikyam [2], J. Kotaiah [3], N. Venkatesh[4], B. Naresh [5]

Abstract

When nonlinear amplifiers are pushed to the point of saturation in satellites, the resulting distortion of the sent signal makes it difficult to receive. However, the M-ray quadrature amplitude modulation (M-QAM) constellation's symmetries are maintained by the nonlinearities induced by memoryless bandpass amplifiers. In this work, we offer a cluster-based sequence equalizer (CBSE) that makes use of these regularities. When compared to more traditional methods like linear transversal equalizers, Volterra equalizers, and RBF network equalizers, the suggested equalizer shows substantial improvement. This performance boost is achieved at a far reduced computational cost as well.

INTRODUCTION

A satellite's job is to operate as a basic repeater, picking up a signal from an earth station or another satellite (uplink) and sending it on to another earth station or another satellite (downlink) [1]. In order to get the most out of the satellite communication system's on-board resources, it's common to push a high power amplifier (HPA) like the travel ing wave tube amplifier (TWTA) to the brink of saturation, which distorts the signal and makes the link nonlinear as a whole. Constant modulus constellation symbols (e.g., 4- QAM) are often utilized to combat nonlinear distortions [2]. However, anytime great band width efficiency is desired [3], massive QAM sig nal constellations must be utilized, which leads to severe nonlinear distortions. For such scenarios, (a) equalization [4, 5] and (b) predistortion or power amplifier linearization [6-8] have been offered as potential solutions to the issue of accurate reception of the broadcast signal. Through equalization, nonlinear (amplifier) and linear (mul tipath) aberrations in the connection are post-cancelled by processing the signal at the receiver to retrieve the sent data. Nonlinear equalizers attempt to balance out the nonlinear effects of the HPA in addition to combating the intersymbol interference (ISI) caused by the propagation channel. The equalization method has the fundamental problem of increasing the financial and computational burden on each terminal. Data is predistorted before the amplifier stage in an effort to replicate the inverse of the amplifier's characteristic and cancel out the nonlinear effects. As a result, the entire pattern becomes linear. The benefit of this method over utilizing an equalization in each terminal is that just a single system is required to cancel the HPA non linearity at the satellite. However, the fundamental problem is that it cannot be used with currently orbiting satellites since the predistorter must be on-board. In addition, a terminal equalizer is still required if multipath is present. Only the first method, equalization on the receiving end, will be discussed in this work. Nonlinear equalizers using NN structures [5, 9] or Volterra series [10, 12] are often used in related works. Multilayer perceptron's (MLP) [13, 14], radial basis functions (RBF) [15, 16], and self-organizing maps (SOM) [17-19] are only few examples of NN-based equalizers. In [20], the efficacy of MLP, RBF, and SOM equalizers is compared. However, NN and Volterra approaches have the drawback of always needing a large (sometimes unrealistic) number of training samples to result in a satisfying solution [5, 11], in addition to their significant computational and implementation complexity.

Assistant Professor[12,3,4,5,]
Mail Id : ram.eee26@gmail.com ,Mail Id : rajarao8200@gmail.com, Mail id : jupellikotaiah@gmail.com ,Mail Id venkatesh.nallamothu1@gmail.com ,Mail Id : naresh.basavoju@gmail.com.
Department of EEE,
Swarna Bharati Institute of Science and Technology (SBIT),
Pakabanda Street,Khammam TS, India-507002.

INTERNATIONAL JOURNAL OF PURE AND APPLIED SCIENCE & TECHNOLOGY
IJPAST

ISSN 2229-6107www.ijpast.in
Vol 12 Issue 1 Mar 2022

EXPLANATION OF THE CHANNEL MODEL AND COMMUNICATIONS SYSTEM

shows how a common satellite communication system [1] works. Historically, communication satellites have used simple transponder relay configurations like the bent-pipe4. Newer satellites include regenerative payloads [2, 28] with on-board processing to keep up with the increasing complexity of mobile global communication networks. This allows for uplink and downlink to be handled independently since the base band broadcast signal is accessible on-board thanks to demodu lation. The suggested equalizer will be used in the down link communication. The downlink communication paradigm is shown in Figure 2(a). Assuming independence and isotropy, the digital signal to be sent is the data stream u + jv. Square root raised cosine (SRRC) filters with enough band width relative to the signal bandwidth are used as the pulse shaping filter just before the memoryless nonlinearity of the HPA. As a result, nonlinearity-following filters are the sole means through which ISI may be introduced [11, 31]. Rectangular M-QAM has been chosen as the preferred signalling technique. The downlink baseband discrete equivalent com medication system model is shown in Figure 2(b), where xk is the kth transmitted symbol that may take on one of M possible values from a source alphabet.

S (S = {a + jb | a, b = (2m−1− √ M) · d, m = 1, 2, ... , √ M} in M-QAM), zk is the

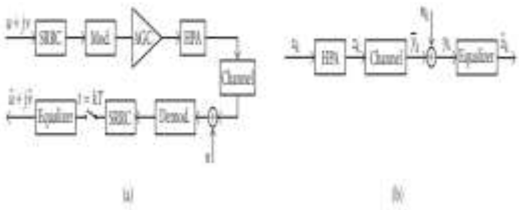

Figure 1: (a) The downlink communication system model and (b) its discrete equivalent.

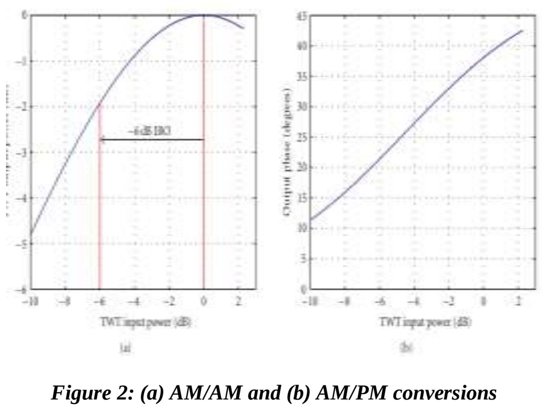

Figure 2: (a) AM/AM and (b) AM/PM conversions

the same symbol at the nonlinear amplifier's output, nk is additive white Gaussian noise that is independent of the channel input, yk is the kth observation that was received, and x k is the symbol that was picked up. Satellites use either traveling wave tube amplifiers (TWTA) or solid-state power amplifiers (SSPA) for their high power ampli fiers (HPA).

(I) TWTA may be thought of as essentially memoryless. Like the ones shown in Figure 3, they are characterized by an AM/AM conversion and an AM/PM conversion. A Saleh model [21] is often used to simulate them.

Memory is included into SSPA (ii). Common approaches to modelling SSPAs with memory use a memoryless nonlinearity (for details on the kind of nonlinearity, see [32]) followed by a linear IIR filter [6].

The One-Dimensional Cluster Sequence Equalizer

Considering a channel model in which the HPA component of our system (Figure 2) is removed, we will quickly go through the 1D CBSE provided in [22], for linear channels. The approach suggested in [22] is an MLSE equalizer that avoids the channel identification step by taking use of the channel's linearity and the symmetries in the source constellation to achieve ML performance with less effort. In order to estimate the ML input sequence, the MLSE equalizer must first calculate an estimate, h, of the CIR and then use the VA (or a version of it) to do so using distances of the form7 Dx = |y h Tx|2. Computing the ML convolution sums h Tx for each of the ML combinations x of L symbols from the alphabet S is time-consuming and computationally expensive for each received sample. It is the set of values y = h Tx that is required in the VA, and not the CIR itself, which is the essential principle behind the 1D CBSE method; in fact, Dx = |y y |2. In addition, these values coincide with the spots (centers) around which the noisy observations cluster because of the noise, therefore they are the noiseless channel outputs. As a result, supervised clustering may be used to directly estimate them. The strength of the noise determines how far apart the clusters are. The number and values of the CIR taps determine both the total number of clusters and where those clusters lie in the complex plane. Since MLSE equalizers need explicit CIR estimation, this means that we may avoid this issue by instead estimating

INTERNATIONAL JOURNAL OF PURE AND APPLIED SCIENCE & TECHNOLOGY
IJPAST

ISSN 2229-6107www.ijpast.in
Vol 12 Issue 1 Mar 2022

the ML centers y of the clusters generated in the complex plane. What's more, by taking use of the constellation symmetry, direct (from the data) estimates for just L carefully selected cluster cen ters sufficient to provide the estimates for all ML of them. 6 Superscript T signifies transposition.

MEMORYLESS NONLINEARITIES AND THE USE OF CONSTELLATION SYMMETRIES

Here, we'll discuss how to apply the previously discussed equalization technique to situations in which a TWTA (as in (3) or (4)) is present. To achieve this goal, we must first define how the nonlinearity influences the input constellation.

Symmetries in the constellations

Rectangular M-ary QAM, the chosen signalling technique, may be thought of as a hybrid of digital amplitude modulation and digital phase modulation. Based on equations (1)–(4), we can write down the baseband complex envelope of the TWTA output as

$$\begin{aligned}\tilde{z}(t) &= g[A(t)]e^{j\{\theta(t)+\Phi[A(t)]\}}\\ &= \left[A(t)e^{j\theta(t)}\right]\left\{\frac{g[A(t)]}{A(t)}e^{j\Phi[A(t)]}\right\}\\ &\triangleq \tilde{x}(t)G(|\tilde{x}(t)|),\end{aligned}$$

where ∼ denotes complex envelope. In words, the output of the TWTA is the product of the input signal with a factor that depends only on the input amplitude. The result is an amplitude change and a phase rotation of the input signal constellation points. Equation (12) implies that the change is the same for all constellation points that share the same energy level. The M symbols in the input constellation can be grouped in two possible ways (see Figure 4(a) for the example of 16-QAM): (1) in I circles on the complex plane, where I is the number of the energy levels (for the 16-QAM case, I = 3), (2) in M/4 squares (four points in each square) that are centered on the origin. Observe that M/4 points lie in each quadrant of the signal space. Since each of these M/4 points is located at the corner of one of the M/4 squares, all M points can result from such a group of M/4 points via simple $n\cdot\pi/2$ rotations, $1 \leq n \leq 3$. After the application of the (memoryless) nonlinearity, a new

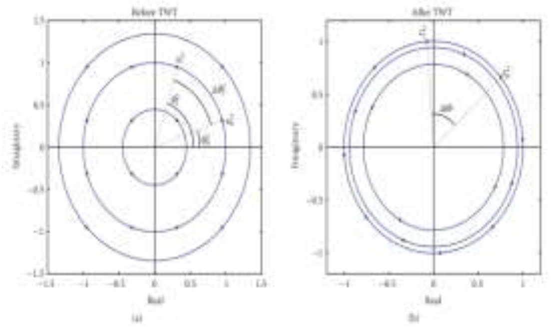

Figure 3: 16-QAM constellation at the (a) input and (b) output of the TWTA.

Equal-angle pairs of modulus symbols are depicted: When = 2 1, the structure of the constellations is established. However, the total number of signal space points remains unchanged (Figure 4(b)). Figure 4 depicts the input (a) and output (b) of the TWTA with identically drawn points and energy levels. It's easy to observe that the amplifier maintains the constellation's symmetry (1, 2). This is because, as shown in Figure 5 and the supplementary material, the angles between the constellation points that share an energy circle do not change. As a consequence, the points that are produced continue to arrange themselves in squares with their centers at the origin, just as they did before the nonlinearity was introduced. Each square's diagonal length is now 2 g(A), and its rotation angle is (A), where A is the amplitude of each of the four symbols on the square's corners, relative to the corresponding square in the input constellation. As a result of the TWTA's nonlinearity, it does not change the total number of energy levels. Next, we'll demonstrate how the CBSE equalizer may make effective use of these symmetry relationships to cut down on the number of cluster centers that must be predicted directly from the training sequence.

EVALUATION IN CONTEXT OF SIMILAR INDICATORS

Here, we evaluate the proposed equalizer against two of the most popular nonlinear equalizers, the Volterra series equalizer (26, 36, 37) and the radial basis function (RBF) equalizer (38, 39), to see how it stacks up. Bit error rates (BER) and computing needs are used to evaluate the methods. It is being considered to use either a 4-QAM or 16-QAM signaling method. We look at a stationary 2-tap (L = 2) channel and an AWGN channel (L = 1). The late ter was selected to mimic real-world situations [5]. The magnitude difference between the first and second taps is 8 dB, and the transfer function is H(z) = (1 0.5j) + (0.3+0.2j)z1. We use the well accepted values for the nonlinearity model parameters in (3), (4) [21]: a = 2.1587, a = 1.1517, p = 4.0033, and p = 9.104. Both the LTE and the Volterra equalizers need 3-dimensional input

INTERNATIONAL JOURNAL OF PURE AND APPLIED SCIENCE & TECHNOLOGY
IJPAST

ISSN 2229-6107www.ijpast.in
Vol 12 Issue 1 Mar 2022

vectors. Since these equalizers were being utilized with minimum-phase channels, the equalization delay was disabled. The stated performance comparisons are representative of the norm across a variety of additional channels.

Linear transversal equalizer

The normalized LMS (NLMS) method [40] was employed in a traditional adaptive linear filter for the LTE. We have determined the optimal step-size,, to minimize mean squared error.

Table 2: Experiment parameters for the LTE and Volterra equalizers (zero equalization delay).

	IBO (dB)	L	LTE	Volterra	
			μ	μ_1	ν
4-QAM	0	1	0.1	0.6	2048
		2	0.1	1.0	512
16-QAM	0	1	0.1	0.7	64
		2	0.1	1.0	256
	−3	1	0.1	0.7	32
		2	0.2	1.2	256
	−6	1	0.1	0.6	32
		2	0.2	1.2	256

each particular case. The corresponding values are given in Table 2.

Volterra equalizer

The output of the Volterra equalizer used in the experiments is given by [37]

$$\hat{x}_n = \sum_i q_i y_{n-i} + \sum_i \sum_j \sum_k q_{i,j,k} y_{n-i} y_{n-j} y^*_{n-k}.$$

Thus, the output of the equalizer consists of a weighted linear and nonlinear combination of channel outputs, with complex weights. Weights qi multiply the channel outputs yn directly, and the weights qi,j,k multiply third-order products of the channel outputs. Only odd-order terms are considered, since even-order terms fall out of the frequency band of interest [26]. The order of the equalizer is restricted to three, because of the prohibitive increase in computational complexity as well as convergence time that higher-order terms would imply. The NLMS algorithm, with different step-sizes for the linear and the nonlinear parts [11], was used to adapt the Volterra weights. The parameters of the algorithm (first-order step-size μ1, third-order step-size μ3) have been chosen so as to optimize the MSE for each case and are given in Table 2. The third-order step-size is related to the first-order step-size as μ3 = μ1/ν

RBF-DF equalizer

The performance of the proposed method is also compared with that of the symbol-by-symbol Bayesian decision feedback (DF) equalizer implemented via an RBF network [38, 39, 41]. A detailed description of the M-ary RBF-DF equalizer, considered here, can be found in [41]. Its structure is specified by the decision delay τ, the feedforward order nf and the feedback order nb. These parameters were chosen in relation to the length of the channel, L, as follows [38, 39, 41]:

$$\tau = L - 1, \qquad n_f = \tau + 1 = L,$$
$$n_b = L + n_f - 2 - \tau = L - 1.$$

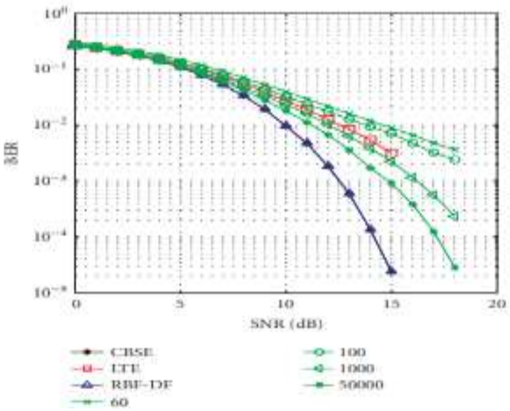

Figure 4 shows the BER performance of the Volterra equalization for a 16-QAM input to an AWGN channel at -6 dB IBO as a function of the duration of the training sequence. We have used training packets with 60, 100, 1000, and 50,000 symbols. The results of the LTE (trained with 100 symbols) and the CBSE and RBF-DF equalizers (trained with 60 symbols) are also shown. The RBF-DF equalizer's M sub-RBF networks have their centers calculated using the recommended CBSE algorithm for fair comparison. In addition, the RBF networks' weights were determined on the basis of the hypothesis that every node's center is equally likely.

Using Simulations for Research

The transmitted symbols are broken down into 500 information symbols and the training symbols. The CBSE and RBF-DF equally use the same training regimen. According to Section 4.3, it is made up of 20 carefully chosen symbols for each energy range. Therefore, the training sequence for 4-QAM (with just one energy zone) consists of 20 symbols, whereas for 16-QAM (with three energy zones), the number of symbols utilized for training is 3 times 20 = 60. The sample size was chosen to be comparable to that utilized in practical systems like GSM [42]. Since there is a trade-off between computational complexity and performance gain,

ISSN 2229-6107www.ijpast.in
Vol 12 Issue 1 Mar 2022

we used just 100 randomly generated symbols in the comparative trials to find the optimal length for the training se quince of the Volterra equalizer. Using an AWGN channel and 16-QAM signalling at 6 dB IBO, Figure 9 provides a detailed comparison of the Volterra equalizer's performance with 60, 100, 1000, and 50000 training symbols. We also utilized 100 randomly generated for the LTE.

Table 3: Real operations required for cluster center estimation.

Relation	Mul/Div	Add/Sub
Equation (22)	$2IL$	$2I(N-L)$
Equation (23)	$2I$	$2I(L-1)$
Equation (24)	$2IL$	$2IL$
Equation (15)	$4L\left(\frac{M}{4}-I\right)$	$2L\left(\frac{M}{4}-I\right)$
Equation (7)	0	$2(L-1)\left[\frac{M^L}{2}-2(L+1)I\right]$
Total	$ML+2I$	$2\left[I(N+1-2L^2) +(L-1)\frac{M^L}{2}+L\frac{M}{4}\right]$

symbols. For each equalizer, the BER is estimated once at least 100 symbol errors have been committed and at least 50 packets have been processed.

CONCLUSIONS

For the specific scenario of rectangular QAM signalling, a cluster-based sequence equalizer for satellite channels has been developed. This method significantly outperforms Volterra and NN-based approaches while incurring much less of a computing burden since TWT memoryless non linearities obey the symmetries underlying the signalling system.

REFERENCES

[1] G. Maral and M. Bousquet, Satellite Communication Systems, John Wiley & Sons, New York, NY, USA, 1996.

[2] M. Ibnkahla, Q. M. Rahman, A. I. Sulyman, H. A. Al-Asady, J. Yuan, and A. Safwat, "High-speed satellite mobile communications: technologies and challenges," Proceedings of the IEEE, vol. 92, no. 2, pp. 312–338, 2004.

[3] F. Xiong, "Modem techniques in satellite communications," IEEE Communications Magazine, vol. 32, no. 8, pp. 84–98, 1994.

[4] E. Biglieri, A. Gersho, R. D. Gitlin, and T. L. Lim, "Adaptive cancellation of nonlinear intersymbol interference for voiceband data transmission," IEEE Journal on Selected Areas in Communications, vol. 2, no. 5, pp. 765–777, 1984.

[5] S. Bouchired, D. Roviras, and F. Castanie, "Equalization of ´ satellite mobile channels with neural network techniques," Space Communications, vol. 15, no. 4, pp. 209–220, 1999.

[6] F. Langlet, H. Abdulkader, D. Roviras, A. Mallet, and F. Castanie, "Comparison of neural network adaptive predistortion ´ techniques for satellite down links," in Proceedings of the International Joint Conference on Neural Networks (IJCNN '01), vol. 1, pp. 709–714, Washington, DC, USA, July 2001.

[7] F. Langlet, D. Roviras, A. Mallet, and F. Castanie, "Mixed ana- ´ log/digital implementation of MLP NN for predistortion," in Proceedings of the International Joint Conference on Neural Networks (IJCNN '02), vol. 3, pp. 2825–2830, Honolulu, Hawaii, USA, May 2002.

[8] F. Langlet, H. Abdulkader, and D. Roviras, "Predistortion of non-linear satellite channels using neural networks: architecture, algorithm and implementation," in Proceedings of the 11th European Signal Processing Conference (EUSIPCO '02), Toulouse, France, September 2002.

[9] S. Haykin, Neural Networks: A Comprehensive Foundation, Prentice-Hall, Upper Saddle River, NJ, USA, 2nd edition, 1999.

[10] A. Gutierrez and W. E. Ryan, "Performance of adaptive Volterra equalizers on nonlinear satellite channels," in IEEE International Conference on Communications (ICC '95), vol. 1, pp. 488–492, Seattle, Wash, USA, June 1995.

[11] A. Gutierrez and W. E. Ryan, "Performance of Volterra and MLSD receivers for nonlinear band-limited satellite systems," IEEE Transactions on Communications, vol. 48, no. 7, pp. 1171– 1177, 2000.

[12] S. Benedetto, E. Biglieri, and R. Daffara, "Modeling and performance evaluation of nonlinear satellite links—a Volterra series approach," IEEE Transactions on Aerospace and Electronic Systems, vol. 15, no. 4, pp. 494–507, 1979.

[13] P.-R. Chang and B.-C. Wang, "Adaptive decision feedback equalization for digital satellite channels using multilayer neural networks," IEEE Journal on Selected Areas in Communications, vol. 13, no. 2, pp. 316–324, 1995.

[14] S. Chen, G. J. Gibson, C. F. N. Cowan, and P. M. Grant, "Adaptive equalization of finite non-linear channels using multilayer perceptrons," Signal Processing, vol. 20, no. 2, pp. 107–119, 1990.

[15] I. Cha and S. A. Kassam, "Channel equalization using adaptive complex radial basis function networks," IEEE Journal on Selected Areas in Communications, vol. 13, no. 1, pp. 122–131, 1995.

[16] S. Chen, S. McLaughlin, and B. Mulgrew, "Complex-valued radial basis function network, part 1: network architecture and learning algorithms," Signal Processing, vol. 35, no. 1, pp. 19– 31, 1994.

[17] S. Bouchired, M. Ibnkahla, and W. Paquier, "A combined LMS-SOM algorithm for time varying non-linear channel equalization," in Proceedings of the European Signal Processing Conference (EUSIPCO '98), Rhodes, Greece, September 1998.

[18] S. Bouchired, M. Ibnkahla, D. Roviras, and F. Castanie,´ "Equalization of satellite mobile communication channels using combined self-organizing maps and RBF networks," in Proceedings of the International Conference on Acoustics, Speech, and Signal Processing (ICASSP '98), vol. 6, pp. 3377–3379, Seattle, Wash, USA, May 1998.

[19] T. Kohonen, Self-Organizing Maps, Springer, Berlin, Germany, 1995.

[20] S. Bouchired, M. Ibnkahla, D. Roviras, and F. Castanie,´ "Equalization of satellite UMTS channels using neural network devices," in Proceedings of the IEEE International Conference on Acoustics, Speech and Signal Processing (ICASSP '99), Phoenix, Ariz, USA, March 1999.